

## Article

# Dependence of atomic thickness on interfacial conditions and magnetocrystalline anisotropy in SmCo<sub>5</sub>/Sm<sub>2</sub>Co<sub>17</sub> multilayer

Soyoung Jekal <sup>1,2†</sup> ,\*<sup>1</sup> Laboratory of Metal Physics and Technology, Department of Materials, ETH Zurich, 8093 Zurich, Switzerland<sup>2</sup> Condensed Matter Theory Group, Paul Scherrer Institute, CH-5232 Villigen PSI, Switzerland

\* Correspondence: so-young.jekal@mat.ethz.ch; Tel.: +41 44 632 26 43

**Abstract:** We have performed first-principles calculations to study the interfacial exchange coupling and magnetocrystalline anisotropy (MCA) energy in a SmCo<sub>5</sub>/Sm<sub>2</sub>Co<sub>17</sub> multilayer model systems. The phase of SmCo<sub>5</sub> and Sm<sub>2</sub>Co<sub>17</sub> stacking along (0001) direction are structurally well matched. The atomic structure, including the alignment and the separation between layers, were firstly optimized. Then the non-collinear magnetic structures were calculated to explore the exchange coupling across the interface and the variation of MCA energy. We found that the inter-phase exchange coupling strength, rotating behavior and MCA energy are strongly dependent on the atomic thickness of the SmCo<sub>5</sub> and Sm<sub>2</sub>Co<sub>17</sub> phase.

**Keywords:** First principles; Exchange energy; magnetocrystalline anisotropy

## 1. Introduction

Since Kneller and Hawig's pioneering work[1] on nanocomposite permanent magnetic materials, which consist of a mixture of hard and soft magnetic phases, exchange coupled permanent magnets have been extensively studied to achieve high maximum energy product values.[2–5]. Interestingly, their demagnetization curves show a shape like those of typical single-phase materials, although these materials consist of, at least, two ferromagnetic phases.[6,7] The single-phase behavior as well as the remanence enhancement have been well understood by taking into account exchange coupling between the small grains of the magnetic phases.[1] So far, many remanence-enhanced magnets based on nanocrystalline mixtures of the hard and soft phases have been found[8–10], and the maximum energy product values have been expected to be enhanced in these hard/soft composite systems, by combining large anisotropy of a hard phase and high saturation magnetization of a soft phase.[11]

Among the commonly used magnetic materials, SmCo<sub>5</sub> has the largest anisotropy energy of 17.2 MJ/m<sup>3</sup> with high Curie temperature of about 1000 K, while 3d-transition metals such as Fe, Co, Ni and their alloys have very high Curie temperatures with large saturation magnetizations.[12] Not only in magnetically hard/soft phases, results of a comparative study on remanence enhanced powders consisting of two magnetically hard phases, SmCo<sub>5</sub> and Sm<sub>2</sub>Co<sub>17</sub> is presented. Similar to those of nanocomposites consisting of soft and hard phases, both the spring-magnet behavior and exchange coupling were observed in the mixtures of these two magnetically hard phases. High coercivity can be obtained in the mechanically alloyed SmCo powders[13] and nanostructured Sm<sub>2</sub>Co<sub>17</sub>-based powders synthesized by reactive milling as well as mechanically milling have been studied systematically.[14,15]

Since Sm<sub>2</sub>Co<sub>17</sub> has both a high Curie temperature and a high magnetocrystalline anisotropy[16–19] which is unobtainable in the 3d-transition metal alloys, it is an important material system to overcome magnetically hard/soft mixtures.

According to early models by Kneller[1] an ideal hard/soft phase multilayer achieves maximum energy product at the optimum thickness of the soft phase which is equal to two domain wall thickness in the hard phase (~ 7 nm for SmCo<sub>5</sub>). However, many recent experimental and theoretical studies

show the important effect of the soft phase parameters and interface conditions.[20–24] Thus it is important to understand the influence of these factors in the inter-phase exchange coupling, in order to achieve better energy products. These issues can be tackled in the scope of first-principles electronic structure calculations based on Density Functional Theory (DFT) as demonstrated in previous works.[25,26]

In the present work, we focused on the effects of the atomic thickness on the interface conditions and the magnetocrystalline anisotropy (MCA) energy in layered  $\text{SmCo}_5/\text{Sm}_2\text{Co}_{17}$  system using first-principles methods. We show that MCA and exchange coupling on the interface between the hard ( $\text{SmCo}_5$ ) and soft ( $\text{Sm}_2\text{Co}_{17}$ ) phase can be modified by atomic thickness of  $\text{SmCo}_5$  and  $\text{Sm}_2\text{Co}_{17}$  layers.

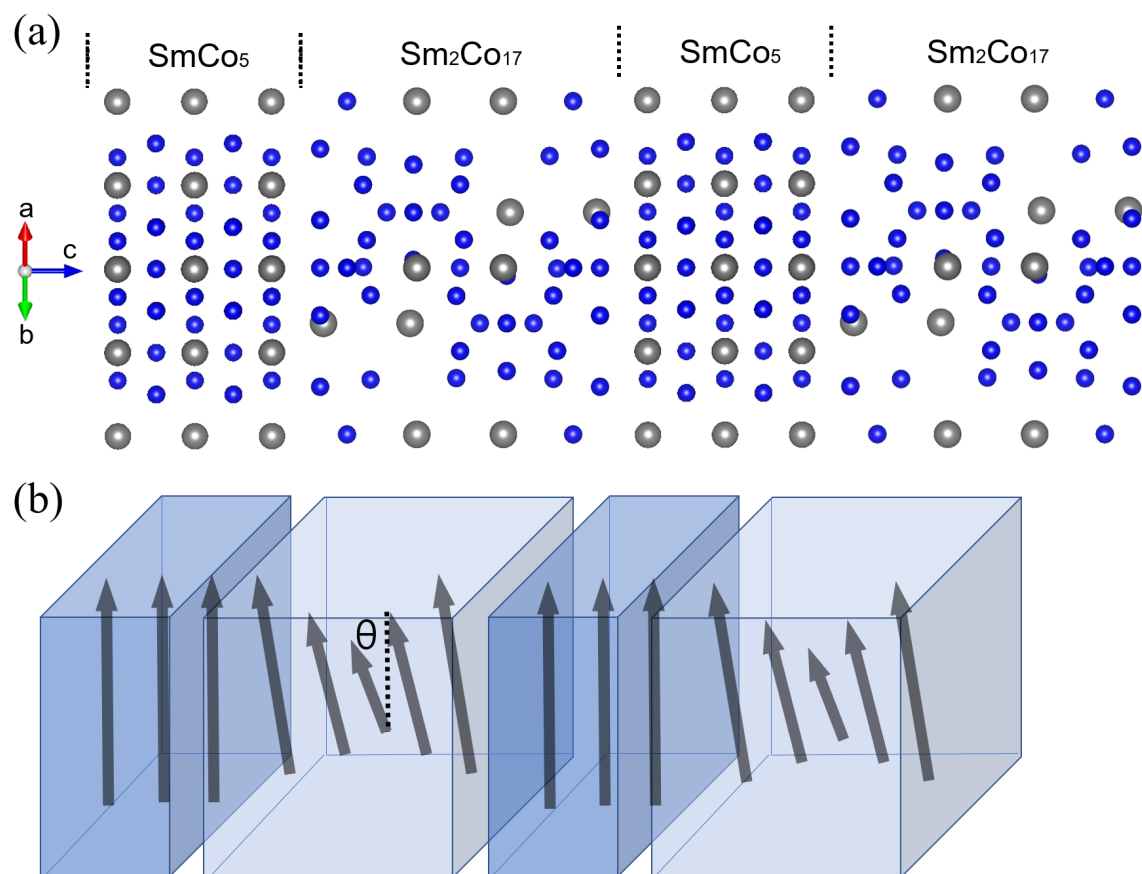


**Figure 1.** (a) Atomic configurations of the two phase superlattice system. The hard ( $\text{SmCo}_5$ ) and soft ( $\text{Sm}_2\text{Co}_{17}$ ) phases are aligned along (0001) direction. The gray large, blue small balls represent Sm and Co atoms, respectively. The dotted lines on top of panel indicate the interface between two phases. The periodic boundary condition has been used. (b) A schematic diagram of non-collinear magnetic orderings in the systems. The arrows represent the directions of magnetic moments of the atoms in each layer.  $\theta$  is the angle between the directions of magnetic moments of the atoms in the hard phase and those in the middle layer of the soft phase, which are fixed.

## 2. Methods

Density Functional Theory (DFT) calculations were mainly performed using plane-wave basis sets and pseudopotentials, implemented in Quantum Espresso (QE) [27], which enables time-efficient calculations.

DFT calculations were performed on superlattice of the  $\text{SmCo}_5/\text{Sm}_2\text{Co}_{17}$  with various atomic thickness. For the exchange-correlation potential we adapted the local spin-density approximation plus Hubbard  $U$  (LSDA+ $U$ ), which can adequately describe the strongly correlated electronic states of

4f electrons [28–30]. Since the LSDA+U method requires the Coulomb energy ( $U$ ) and the exchange energy ( $\mathcal{J}$ ) as input parameters,  $U$  and  $\mathcal{J}$  were defined through the derivatives of the energy levels  $\epsilon_f$  of the  $f$ -orbital with respect to their occupancies  $n_f$ , described as  $U = \partial\epsilon_{f\uparrow}/\partial n_{f\downarrow}$  and  $\mathcal{J} = \partial(\epsilon_{f\uparrow} - \epsilon_{f\downarrow})/\partial(n_{f\uparrow} - n_{f\downarrow})$  for the majority (minority) spin  $\uparrow$  ( $\downarrow$ ), respectively. From these expressions we obtain  $U = 6.0$  eV and  $\mathcal{J} = 1.0$  eV for Sm.

The wave functions were expanded by a plane-wave basis set with an optimized cutoff energy of 340 Ry, and the Brillouin zone was sampled via a  $12 \times 12 \times 4$   $k$ -point mesh. Different mesh values from 72 to 980 were tested to ensure the precise of our calculations, with the convergence criterion being 0.1 eV. The convergence with respect to cutoff was also carefully checked.

## 2.1. Atomic structure

The superlattice model is adopted to construct the interface structure for our simulation. A superlattice consists of SmCo<sub>5</sub> and Sm<sub>2</sub>Co<sub>17</sub> layers stacking along (0001) direction as shown in Figure 1(a). Lattice constants of SmCo<sub>5</sub> and Sm<sub>2</sub>Co<sub>17</sub> have a mismatch of 17% along this direction. To optimize the atomic structure, the self-consistent spin-polarized electronic structure calculations with periodic boundary conditions was carried out with fully relaxation.

## 2.2. Exchange coupling

We consider the exchange-spring multilayer with the size of the hard and soft layer smaller than the thickness of a usual domain wall, therefore, the exchange-coupling between the two phases will be in effect. A single domain case is considered for both the hard and the soft phase in the present modeling interface. To describe the exchange coupling strength between the soft and hard phases, we model a simulated demagnetization process of the magnetic systems using non-collinear magnetic structure calculations. In this method we rotate the direction of local magnetic moments at the center of soft layer from ferromagnetic to a finite angle. We vary this angle as a parameter to extract the strength of the interlayer exchange coupling. This result is double-checked by using a perturbative method.

## 2.3. Magnetocrystalline anisotropy energy

The magnetocrystalline anisotropy energy  $E_{\text{MCA}}$  was calculated using the force theorem. It is defined as the total energy difference between the magnetization perpendicular to the [1000]-plane and in the [1000]-plane of the SmCo<sub>5</sub> and Sm<sub>2</sub>Co<sub>17</sub> structures, i.e.,  $K = E_{[100]} - E_{[001]}$ , where  $E_{[1000]}$  and  $E_{[0001]}$  are the total energies with the magnetization aligned along the hard- ([1000]) and easy-axis ([0001]) of the magnetic anisotropy, respectively. Specifically,  $E_{\text{MCA}}$  is calculated in three steps: first, collinear self-consistent calculation is performed without spin-orbit coupling (SOC); second, the density matrix is globally rotated to consider the magnetization along [1000] and [0001] to calculate  $E_{[1000]}$  and  $E_{[0001]}$ ; and finally, non-collinear and non-self-consistent calculation is performed with SOC.

## 3. Results

### 3.1. Atomic structures & magnetic moments

We firstly found the equilibrium structural parameters of considered superlattices. Atoms were fully relaxed along c-direction while the in-plane lattice parameter  $a_{in}$  is fixed to  $8.367 \text{ \AA} \leq a \leq 9.834 \text{ \AA}$ . In the optimized structures, we investigated average magnetic moments of each layers of superlattices which consist different thickness of hard and soft phases. Fig. 2(a) and (b) present calculated in-plane lattice constants and magnetic moments. Since in-plane lattice constant (2x2) SmCo<sub>5</sub> is 17% larger than (1x1) Sm<sub>2</sub>Co<sub>17</sub>, in-plane lattice constant is getting increase with thicker SmCo<sub>5</sub> and thinner Sm<sub>2</sub>Co<sub>17</sub>, as expected. Regardless of atomic thickness, interface atoms between soft and hard phase show noticeably

large magnetic moments compared to the that of centered atoms. The magnetic moment gradually decreased from the interface to the center, especially in the soft phase.

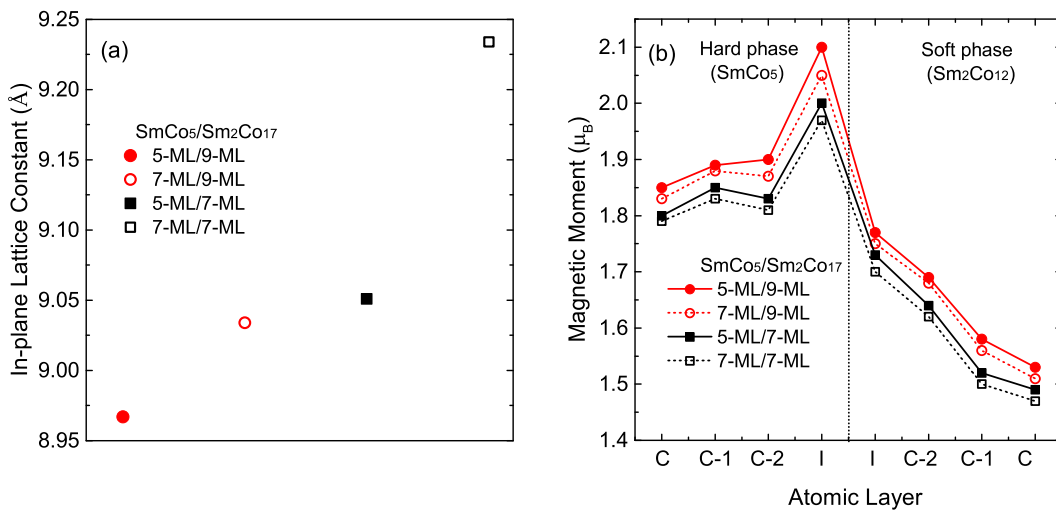


**Figure 2.** (a) The optimized in-plane lattice constant of the supercells. (b) Calculated average magnetic moment of Co atoms with respect to the atomic layer. C and C-n denote the centered layer and the n layer below the center, respectively. I denote the interface.

### 3.2. Exchange energies

An important issue for assessing the applicability of exchange-spring magnets is the nature of the magnetic reversal processes. To address this problem, the optimized structure is used as an input for non-collinear magnetic order calculations using The full-potential linear muffin-tin orbital (FP-LMTO) method[31]. Our model mimics a domain wall which forms in the demagnetization process. We consider the directions of the magnetic moments of the atoms in the hard phase were fixed to the easy magnetization axis direction and seven or nine layers of soft phase with magnetic moments rotated from its FM order as illustrated in Figure 1(b). The magnetic moments of atoms in the middle layer of the soft phase were fixed to turn a given angle  $\theta$  relative to the direction of the magnetic moments of the hard phase, while the magnetic moments of other atoms in the soft phase were free to relax. Upon the convergence of the calculations is reached, the total energy is obtained for each given angle  $\theta$ . The total energy difference for the system,  $\delta E(\theta) = E(\theta) - E(\theta=0^\circ)$ , as a function of the turning angle  $\theta$  is shown in Fig.3(a).

We find that  $\delta E(\theta)$  behaves as a quadratic function of  $\theta$ , manifesting the spring behavior and the exchange coupling between the soft and hard phases in this system. We compare results in the case of the hard and soft phases made of different atomic thickness. The systems with thinner hard phase and thicker soft phase are expected to strengthen the exchange coupling. In Ref.[32], they demonstrated a reduced exchange energy at interface by showing the variation of the layer resolved angle of rotations of atomic moment across the soft phase. Exchange coupling energy is the strongest between the centered layers of soft phases, but weakest across the interface.

Interestingly, we find the considerable effect of atomic thickness of superlattice on the exchange coupling at interface. As shown in Fig.3,  $\delta E(\theta)$  is a quadratic function of  $\theta$  for whole systems. However, the curve of system with thinner hard phase and thicker soft phase is much steeper, indicating that the exchange coupling in this system is stronger than the other candidates. Comparing relaxed angles of magnetic moment, we observe smaller angle of rotation in the interface layer while angle of centered layers of soft phase is fixed as 45°.

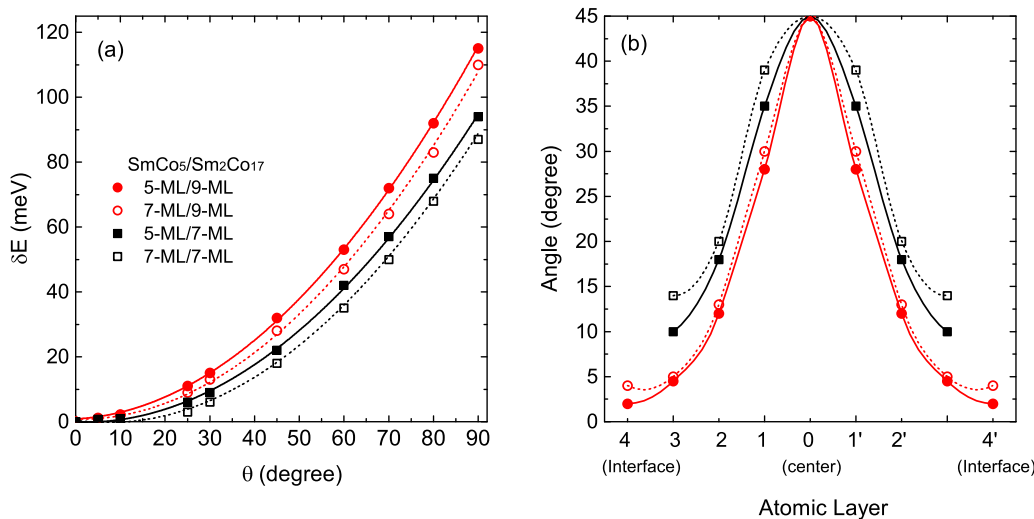


**Figure 3.** (a) The calculated total energy differences,  $\delta E(\theta) = E(\theta) - E(\theta=0^\circ)$  and their fitting to a quadratic curve for the four systems with various atomic thickness. (b) The angle distributions for the soft phase atomic layers parallel to the interface plane (refer to Fig.1). 0 label represent centered layer which is the middle layer of the soft phase, whose atomic magnetic moments are turned at a fixed value of  $45^\circ$  away from those in the hard phase layers. All the atomic magnetic moment orientation in layers 1 (1'), 2 (2'), 3 (3'), and 4 (4') are obtained self-consistently.

To further understand the phenomena, we have calculated the site-to-site exchange interaction parameters  $J_{ij}$  between sites  $i$  and  $j$ ,

$$J_{ij} = \frac{1}{4\pi} \times \int_{-\infty}^{E_F} d\epsilon \sum_{m_i, m_j, m_i', m_j'} \text{Im}[\Delta_i^{mm'} G_{ij\downarrow}^{m'm''}(\epsilon) \Delta_j^{m''m'''} G_{ij\uparrow}^{m'''m}(\epsilon)], \quad (1)$$

where  $\Delta_i^{mm'} = \int_{\text{BZ}} [H_{ii\uparrow}^{mm'}(k) - H_{ii\downarrow}^{mm'}(k)] dk$  is the exchange splitting within the Brillouin zone and  $G_{ij\downarrow}^{m'm''}(\epsilon)$  is the real-space Green's function.

Since  $J_{ij}$  decreases rapidly as a function of the distance, the calculation is limited to the few nearest neighboring pairs only. The  $J_{ij}$  for pairs across the hard/soft interface are averaged over the atomic pairs between the two layers and the results for the four models of 3-ML/9ML, 5-ML/9ML, 3-ML/7ML, and 5-ML/7ML, are 130.01, 129.83, 124.76, 122.45 meV, respectively, in the ferromagnetic state. It is clear that the absolute values of site-to-site exchange parameters of the interface atomic pairs in system 3-ML(SmCo<sub>5</sub>)/9-ML(Sm<sub>2</sub>Co<sub>17</sub>) are larger than those of the corresponding pairs in other candidate systems. This also supports that the inter-phase exchange coupling in system with thinner hard phase and thicker soft phase is stronger, in agreement with the present non-collinear magnetic order calculation as discussed above.

### 3.3. Magnetocrystalline anisotropy

For the magnetocrystalline anisotropy, we also find a atomic thickness dependency. In fact, for 5-ML/9-ML the anisotropy energy is  $\sim 2.3$  meV/atom, which is 35% larger than that of bulk SmCo<sub>5</sub> ( $\sim 1.5$  meV/atom)[33]. However, it decrease in the systems with thicker hard phase or thinner soft phase, due to the increased symmetry.

Even if this system is a superlattice with broken symmetry unlike a bulk SmCo<sub>5</sub>, the 35% enhancement in  $E_{\text{MCA}}$  for 5-ML/9-ML is unexpected. As shown in Fig. 4(b), the main contribution to the enhancement of  $E_{\text{MCA}}$  comes from the interface between hard and soft phases. The origin of large MCA is ascribed to the spin-orbit induced mixing between 4f and 3d orbitals at the interface between the hard and soft phases.

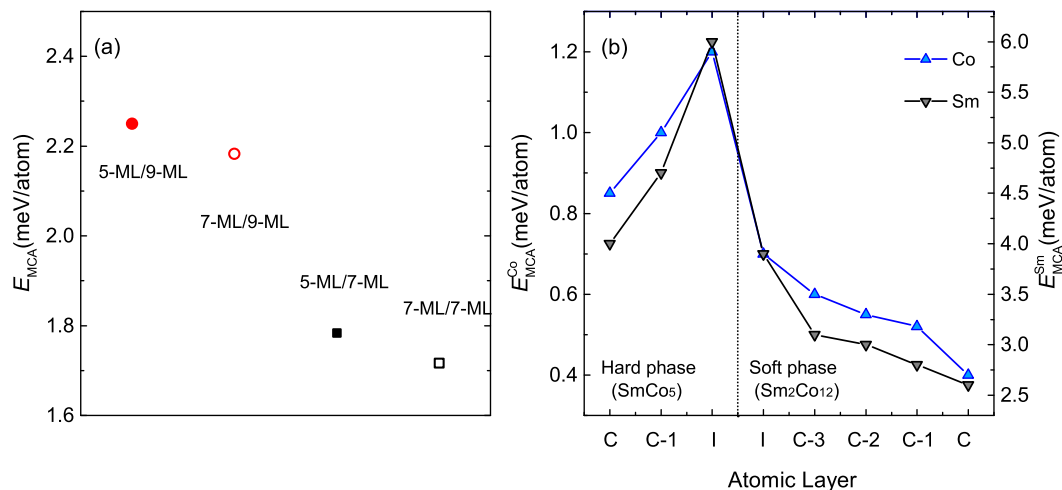


**Figure 4.** (a) Magnetocrystalline anisotropy energy ( $E_{MCA}$ ). (b) Partial  $E_{MCA}$  of Co and Sm with respect to the atomic layer of 5-ML/9-ML superlattice.

#### 4. Conclusions

In conclusion, we have carried out first-principles calculations of the MCA energy and the exchange coupling across SmCo<sub>5</sub>/Sm<sub>2</sub>Co<sub>17</sub> multilayers. Using both the non-collinear magnetic structure simulation and the calculation of the site-to-site exchange parameters across the interfaces, we found that the exchange coupling in SmCo<sub>5</sub>/Sm<sub>2</sub>Co<sub>17</sub> is enhanced by the thin (<5-ML) hard phase and thick (>9-ML) soft phase. This system also shows the strongest MCA energy among other candidates we considered, and the most contribution comes from the interface between hard and soft phases. The origin of large MCA is ascribed to the spin-orbit induced mixing between 4f and 3d orbitals at the interface between the hard and soft phases.

1. Kneller, E.F.; Hawig, R. The exchange-spring magnet: a new material principle for permanent magnets. *IEEE Transactions on Magnetics* **1991**, *27*, 3588–3560.
2. Bader, S.D. Colloquium: Opportunities in nanomagnetism. *Reviews of modern physics* **2006**, *78*, 1.
3. Lopez-Ortega, A.; Estrader, M.; Salazar-Alvarez, G.; Roca, A.G.; Nogues, J. Applications of exchange coupled bi-magnetic hard/soft and soft/hard magnetic core/shell nanoparticles. *Physics Reports* **2015**, *553*, 1–32.
4. Jiang, J.; Bader, S. Rational design of the exchange-spring permanent magnet. *Journal of Physics: Condensed Matter* **2014**, *26*, 064214.
5. Cui, W.; Sepehri-Amin, H.; Takahashi, Y.; Hono, K. Hard magnetic properties of spacer-layer-tuned NdFeB/Ta/Fe nanocomposite films. *Acta Materialia* **2015**, *84*, 405–412.
6. Müller, K.H.; Schneider, J.; Handstein, A.; Eckert, D.; Nothnagel, P.; Kirchmayr, H. Comparison of melt-spun Nd 4 Fe 77 B 19 with neodymium-rich isotropic permanent magnets. In *Rapidly Quenched Materials*; Elsevier, 1991; pp. 151–153.
7. Eckert, D.; Müller, K.; Handstein, A.; Schneider, J.; Grossinger, R.; Krewenka, R. Temperature dependence of the coercive force in Nd<sub>4</sub>Fe<sub>77</sub>B<sub>19</sub>. *IEEE Transactions on Magnetics* **1990**, *26*, 1834–1836.
8. Manaf, A.; Buckley, R.; Davies, H. New nanocrystalline high-remanence Nd-Fe-B alloys by rapid solidification. *Journal of Magnetism and Magnetic Materials* **1993**, *128*, 302–306.
9. Ding, J.; McCormick, P.; Street, R. Remanence enhancement in mechanically alloyed isotropic Sm<sub>7</sub>Fe<sub>93</sub>-nitride. *Journal of magnetism and magnetic materials* **1993**, *124*, 1–4.
10. Zheng, B.; Zhang, H.W.; Zhao, S.f.; Chen, J.l.; Wu, G.h. The physical origin of open recoil loops in nanocrystalline permanent magnets. *Applied Physics Letters* **2008**, *93*, 182503.
11. Zhang, J.; Takahashi, Y.; Gopalan, R.; Hono, K. Sm (Co, Cu) 5 / Fe exchange spring multilayer films with high energy product. *Applied Physics Letters* **2005**, *86*, 122509.

12. Skomski, R.; Coey, J. *Permanent magnetism*; Institute of Physics Pub., 1999.
13. Liu, J.P.; Fullerton, E.; Gutfleisch, O.; Sellmyer, D.J. *Nanoscale magnetic materials and applications*; Springer, 2009.
14. Duerrschnabel, M.; Yi, M.; Uestuener, K.; Liesegang, M.; Katter, M.; Kleebe, H.J.; Xu, B.; Gutfleisch, O.; Molina-Luna, L. Atomic structure and domain wall pinning in samarium-cobalt-based permanent magnets. *Nature communications* **2017**, *8*, 54.
15. Hiraga, K.; Hirabayashi, M.; Ishigaki, N. High resolution transmission electron microscopy of Sm-Co based permanent magnets. *Journal of Microscopy* **1986**, *142*, 201–210.
16. Zhou, J.; Skomski, R.; Chen, C.; Hadjipanayis, G.C.; Sellmyer, D.J. Sm–Co–Cu–Ti high-temperature permanent magnets. *Applied Physics Letters* **2000**, *77*, 1514–1516.
17. Gutfleisch, O. Controlling the properties of high energy density permanent magnetic materials by different processing routes. *Journal of Physics D: Applied Physics* **2000**, *33*, R157.
18. Gutfleisch, O.; Willard, M.A.; Brück, E.; Chen, C.H.; Sankar, S.; Liu, J.P. Magnetic materials and devices for the 21st century: stronger, lighter, and more energy efficient. *Advanced materials* **2011**, *23*, 821–842.
19. Handstein, A.; Yan, A.; Martinek, G.; Gutfleisch, O.; Muller, K.H.; Schultz, L. Stability of magnetic properties of Sm<sub>2</sub>Co<sub>17</sub>-type magnets at operating temperatures higher than 400/spl deg/C. *IEEE transactions on magnetics* **2003**, *39*, 2923–2925.
20. Shan, Z.; Liu, J.; Chakka, V.M.; Zeng, H.; Jiang, J. Energy barrier and magnetic properties of exchange-coupled hard-soft bilayer. *IEEE transactions on magnetics* **2002**, *38*, 2907–2909.
21. Guo, Z.; Jiang, J.; Pearson, J.; Bader, S.; Liu, J. Exchange-coupled Sm–Co/Nd–Co nanomagnets: correlation between soft phase anisotropy and exchange field. *Applied physics letters* **2002**, *81*, 2029–2031.
22. Asti, G.; Solzi, M.; Ghidini, M.; Neri, F.M. Micromagnetic analysis of exchange-coupled hard-soft planar nanocomposites. *Physical Review B* **2004**, *69*, 174401.
23. Choi, Y.; Jiang, J.; Ding, Y.; Rosenberg, R.; Pearson, J.; Bader, S.; Zambano, A.; Murakami, M.; Takeuchi, I.; Wang, Z.; others. Role of diffused Co atoms in improving effective exchange coupling in Sm–Co/Fe spring magnets. *Physical Review B* **2007**, *75*, 104432.
24. Zambano, A.; Oguchi, H.; Takeuchi, I.; Choi, Y.; Jiang, J.; Liu, J.; Lofland, S.; Josell, D.; Bendersky, L.A. Dependence of exchange coupling interaction on micromagnetic constants in hard/soft magnetic bilayer systems. *Physical Review B* **2007**, *75*, 144429.
25. Sabiryanov, R.; Jaswal, S. Electronic structure and magnetic properties of hard/soft multilayers. *Journal of magnetism and magnetic materials* **1998**, *177*, 989–990.
26. Sabiryanov, R.; Jaswal, S. Magnetic properties of hard/soft composites: SmCo<sub>5</sub>/C<sub>0.1-x</sub>Fe<sub>x</sub>. *Physical Review B* **1998**, *58*, 12071.
27. Giannozzi, P.; et al.. QUANTUM ESPRESSO: a modular and open-source software project for quantum simulations of materials. *Journal of physics: Condensed matter* **2009**, *21*, 395502.
28. Steinbeck, L.; Richter, M.; Eschrig, H. Magnetocrystalline anisotropy of RC<sub>0.5</sub> intermetallics: itinerant-electron contribution. *Journal of magnetism and magnetic materials* **2001**, *226*, 1011–1013.
29. Larson, P.; Mazin, I.; Papaconstantopoulos, D.A. Calculation of magnetic anisotropy energy in SmCo<sub>5</sub>. *Physical Review B* **2003**, *67*, 214405.
30. Larson, P.; Mazin, I.; Papaconstantopoulos, D.A. Effects of doping on the magnetic anisotropy energy in SmCo<sub>5-x</sub>Fe<sub>x</sub> and YCo<sub>5-x</sub>Fe<sub>x</sub>. *Physical Review B* **2004**, *69*, 134408.
31. Mryasov, O.; Sabiryanov, R.; Freeman, A.; Jaswal, S. Effect of lattice distortions on the competition between the double and superexchange mechanisms in LaMnO<sub>3</sub>. *Physical Review B* **1997**, *56*, 7255.
32. Wu, D.; Zhang, Q.; Liu, P.J.; Sabirianov, R.F. Dependence of exchange coupling on interfacial conditions in SmCo<sub>5</sub>/Co system: A first-principles study. *Journal of nanoscience and nanotechnology* **2008**, *8*, 3036–3039.
33. Jekal, S.; Loeffler, J.; Charilaou, M. Pushing the limits of magnetic anisotropy in the Sm–Co system. *arXiv preprint arXiv:1807.09257* **2018**.